Apparent exchange rate of water in human brain matter revealed by a novel pulse sequence

M. Nilsson[1], D. Topgaard[2], S. Brockstedt[3], F. Ståhlberg[1,4], and J. Lätt[1,5]

[1]Department of Medical Radiation Physics, Lund University, Lund, Sweden, [2]Physical Chemistry, Lund University, Lund, Sweden, [3]Radiation Physics, Lund University, Lund, Sweden, [4]Department of Diagnostic Radiology, Lund University, Lund, Sweden, [5]Center for Medical Imaging and Physiology, Lund University Hospital, Lund, Sweden

Introduction

Diffusion MRI using pulsed gradient spin echoes (PGSE) is known to yield information about tissue microstructure; for instance, measurements with different diffusion times (T_D) provide structural information regarding cellular size distributions [1]. Recent studies have shown that exchange may affect PGSE measurements in white matter [2] and in sub-acute stroke lesions [3]. However, cell membrane permeability, i.e. the water exchange rate, is seldom estimated due to the limited sensitivity of the PGSE sequence. A sequence more sensitive to exchange than the PGSE sequence would be desirable to probe the cell membrane permeability, which is expected to be altered for several types of brain pathology [4]. In this study, we employed a novel pulse sequence at an MRI scanner, previously implemented at an NMR spectrometer [5], to measure the apparent water exchange rate in both a phantom and *in vivo*.

Theory

A schematic overview of the sequence is presented in Fig. 1. A diffusion weighted (DW) block precede an ordinary DWI sequence, which selectively attenuate the signal from the fast diffusion component. The diffusion sensitivity from the first pair of gradients is denoted b_f and from the second pair is denoted b, with $b = (\gamma\delta g)^2 T_D$ and $T_D = \Delta\text{-}\delta/3$. To estimate the apparent exchange rate (*AXR*), the apparent diffusion coefficient (*ADC*) was measured using two different b-values in the DWI-block while varying the mixing time (*TM*) and applying a fixed b_f. The equilibrium ADC_{eq} was estimated using a short *TM* (approximately 20 ms) and $b_f = 0$. Analysis was performed using the following equation

$$S = A \cdot \exp\left(-b \cdot ADC_f\right), \qquad ADC_f = ADC_{eq}\left[1 - \sigma \cdot \exp\left(-TM \cdot AXR\right)\right] \tag{1}$$

where A is the signal strength for $b = 0$, ADC_f is the *ADC* after filtering and σ is the filter efficiency, set to zero when $b_f = 0$ and limited to a maximal value of unity. In a two component system with two distinct *ADC*s, $AXR = (1 + f_2/f_1)\, k_1$ where f_1 and f_2 are the volume fractions of the slow and fast diffusion components and k_1 is the exchange rate of the slow diffusion component.

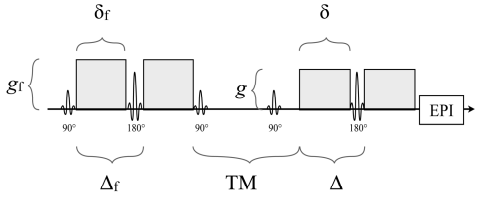

Fig. 1. Illustration of the pulse sequence employed for permeability-sensitive diffusion MRI. A filtering DW block and an adjustable delay of duration *TM* precede a standard DWI sequence. Each DW block contains a pair of diffusion sensitizing gradient pulses of duration δ and amplitude g. The time between the onset of the pulses in the pulse pair is denoted Δ. The filtering block is designed to selectively attenuate the signal from the fast diffusion component.

Method

Measurements were performed at an Philips 3T Acheiva system in a phantom of baker's yeast at room temperature as well as in healthy volunteers. Informed consent was obtained. The *in vivo* measurements were performed with: TE/TR = 97/2500 ms, b_f = 1300 s/mm2, b = 40 and 900 s/mm^2, a voxel size of 3x3x5 mm^3 and *TM* varied between 20 ms and 400 ms in 18 steps. The diffusion encoding direction was (1,1,0). Total scan time was 12 min. The yeast measurements were performed with similar sequence parameters.

Results

In the yeast phantom, the *AXR* was 1.7±0.3 s^{-1} (mean ± standard deviation) and parametric maps of the model parameters ADC_{eq}, σ and *AXR* are shown in Fig. 2. The *in vivo* measurements showed *AXR*-values between approximately 1.0 and 2.5 s^{-1} (Fig. 3).

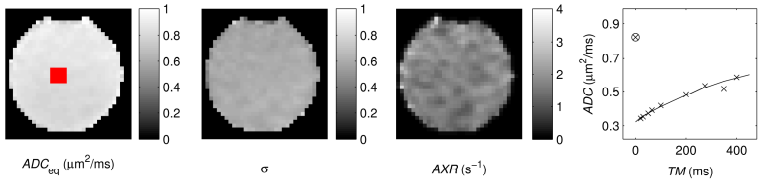

Fig. 2 (above). Parametric maps of ADC_{eq}, σ and *AXR*. The ADC_{eq} decreases slightly from top to bottom due to sedimentation. Rightmost: *ADC* estimated for each *TM* shown by crosses and model fit as a solid line, with data obtained from the ROI shown in red in the ADC_{eq} map.

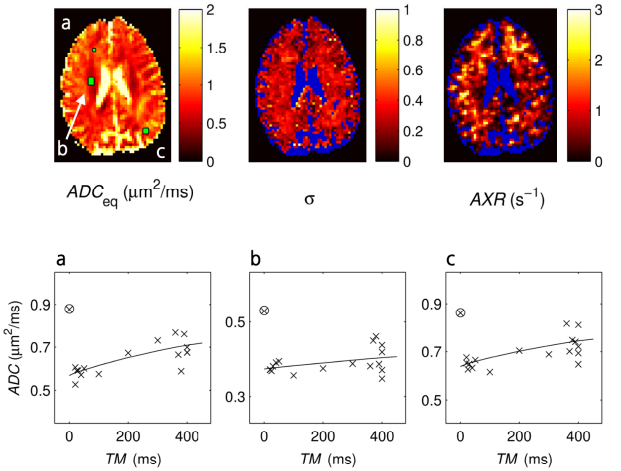

Fig. 3 (right). Top row: Parametric maps of ADC_{eq}, σ and *AXR*. Areas with ADC_{eq} greater than 1.2 μm^2/ms were marked with blue in the σ and *AXR* map. Extreme values in the *AXR* and σ maps, identified by unsuccessful model fits, were replaced by the median of their neighbours. The observed *AXR* was mainly in the range between 1 and 2.5 s^{-1}. Bottom row: The crosses shows that *ADC* increases with *TM*, indicating exchange, with data obtained from ROIs shown in green in the ADC_{eq} map. Model fit is shown as a solid line and the observed *AXR*-values were 1.5, 0.5 and 1.6 s^{-1}.

Discussion and conclusion

A pulse sequence, originally developed for studying cell membrane permeability using an NMR spectrometer [5], was successfully implemented at a clinical MRI scanner. The sequence is sensitive to exchange between water pools with different diffusion coefficients. The results from yeast phantom measurements agreed with previous NMR spectrometry studies [5]. *In vivo* results showed effects of exchange in brain matter. One potential error source is compartmentally different T1-relaxation times, although it is likely of minor influence *in vivo* [6]. Assuming $f_1 = f_2$, the exchange rate k_1 were in the order of 1 s^{-1}, values which would have been inaccessible using a PGSE or PGSTE sequence with varied T_D. The estimated *AXR* is the most noise-sensitive of the estimated parameters and it is not expected to be sensitive to the measurement direction. The signal-to-noise ratio in the deep parts of the brain was approximately half as compared to outer parts of the brain, which might affect the estimated *AXR* in the central brain.

In conclusion, the apparent exchange rate can be estimated *in vivo* using this novel pulse sequence. This is potentially a very useful contrast mechanism in MRI.

References [1] Barazany D, *et al*. Brain 2009:132(5):1210-1220 [2] Nilsson M, *et al*. 2009:27(2):176-187 [3] Lätt J, *et al*. NMR Biomed 2009:22(6):619-628 [4] Tait MJ, *et al*. Trends Neurosci 2007:31:37-43 [5] Åslund I, *et al*. JMR 2009:200:291-295 [6] Mulkern R, *et al.* MRM 2000:44:292-300